CHARON'S EXTREME EXOSPHERIC DYNAMICS AND RED SPOT ORIGINS. Ben Teolis[1,2,3*], Ujjwal Raut[1,2,3], Joshua A. Kammer[2], Caleb J. Gimar[1,2,3], Carly J. A. Howett[4], G. Randall Gladstone[2,3], Kurt D. Retherford[1,2,3], [1]Center for Laboratory Astrophysics and Space Science Experiments (CLASSE), Space Science and Engineering, Southwest Research Institute, San Antonio, Texas, 78238., [2]Space Science and Engineering, Southwest Research Institute, San Antonio, Texas, 78238., [3]Department of Physics and Astronomy, University of Texas at San Antonio, San Antonio, Texas, 78249, [4]Department of Space Studies, Southwest Research Institute, Boulder, Colorado, 80302. *ben.teolis@swri.org

Introduction: Drastic and rapid equinoctial surges in Charon's methane exosphere, over three orders of magnitude in gas density, make its exosphere's seasonal variability some of the most extreme of in the solar system according to our exospheric modeling. Charon's exosphere was below detectability at the time of the New Horizons encounter [*Stern et al.*, 2017], but models show [*Hoey et al.*, 2017; *Tucker et al.*, 2015] that some methane escaping Pluto's atmosphere is gravitationally captured by Charon. We find that Charon's drastic exospheric dynamics, prompted by its extreme seasons and the swift evaporation and refreezing of polar caps of frozen methane from and to Charon's spring at autumn polar zones, may be essential to grasping the origins of Charon's enigmatic polar red spot imaged by the New Horizons MVIC camera. Already suspected to be a product of Ly-α photolysis of frozen polar methane [*Grundy et al.,* 2016], we find by incorporating the photolysis process into our exospheric models, that exposure of photolytic ethane to solar wind may also be a necessary step in generating the red material.

Modeling: The Monte Carlo exospheric simulation [*Teolis and Waite*, 2016] considers the CH_4 arrival flux onto Charon [*Hoey et al.*, 2017], Charon's gravity, CH_4 surface adsorption/desorption, and Ly-α photolysis of surface methane into photoproducts. Simulation molecules stick transiently to the surface and desorb stochastically according to an Arrhenius law and a Maxwell-Boltzmann velocity distribution at the local surface temperature. We model the surface temperature (versus position and time) using the identical approach to *Grundy et al.* [2016]; i.e., using as input the estimated thermal inertia (2.5 - 40 J m-2 K-1 s-1/2), albedo (~0.3) and emissivity (~ 0.9) [*Grundy et al.,* 2016], respectively, and the seasonal time evolution of solar insolation. Ejected molecules are propagated along uninterrupted trajectories before escaping Charon's gravity or falling back to the surface to re-adsorb. Molecules thereby 'hop' in random walk fashion, redistributing around Charon to form evolving surface condensate and exospheric gas distributions.

Results: We show in Figure 1 two snapshots in time of Charon's modeled exospheric gas density distribution a few years before (in 1985) and after (1990) the 16 Dec 1987 equinox. During this time period – exceeding brief compared to the 248 year Pluto-Charon heliocentric orbital period - the exospheric density rises roughly three orders of magnitude, as the sun rises near the northern (spring) pole. As the terminator approached the pole, sublimated methane initially refreezes closer to the pole, in a "pushbroom" effect that shrinks and concentrates the polar cap. However with the loss of the polar night zone near equinox, sublimated methane has nowhere to go but into the exosphere, resulting a brief (roughly 4 earth years) but drastic surge in Charon's entire exosphere.

Almost simultaneous to the disappearance of one polar cap at the spring polar zone, another polar cap condenses out of the surging exosphere onto the autumnal polar zone. This rapidly accreted 'flash frozen' polar cap – several tens of microns thick - persists over the polar winter, and swaps between poles at every equinox. Additionally, with the expansion of the polar night zone over the long Charon winters, several hundred nanometers more methane frost freezes gradually outside of the main polar caps down to lower latitudes, owing to CH_4 continually arriving at Charon from Pluto.

At thicknesses ranging between hundreds of nanometers and tens of microns, the methane frost thickness is well beyond the ~35 nm [*Martonchik and Orton*, 1994] optical depth of Ly-α light. For this reason photo-destruction of methane is not very efficient [*Grundy et al.,* 2016]; we estimate only ~10% of the methane arriving at Charon is converted to more complex hydrocarbons that could contribute to the red material.

An important aspect of the photolysis process at Charon is that CH_4 is continuously being accreted onto the surface, diluting the photolysis products as they are being produced. Laboratory experiments [*Raut et al.*, 2022] duplicating Charon-like conditions of simultaneous methane condensation and Ly-α light exposure suggest ethane to be the primary photoproduct under these conditions. Ethane, being less volatile than methane, may stick to the polar surface past spring equinox, and may under exposure to solar wind be radiolyzed into more complex hydrocarbon refractory 'tholins' that may contribute to the red material.

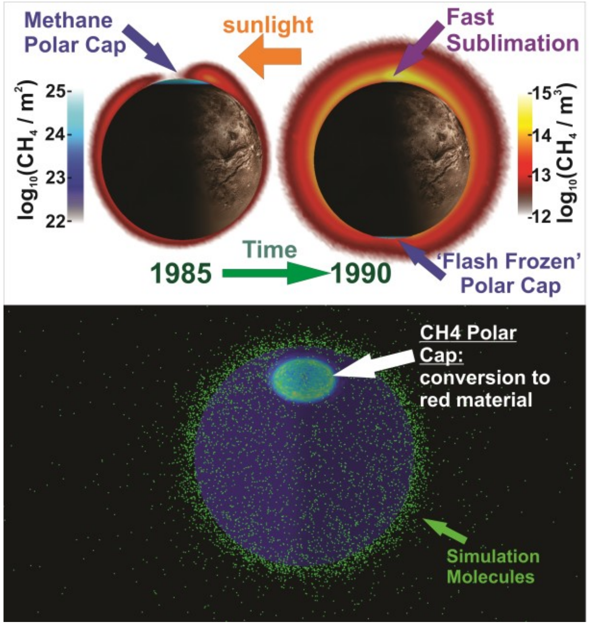

Figure 1. Top: Two snapshots in time of Charon's evolving exospheric gas (red color: CH_4 density cross section) and surface condensate (blue color: CH_4 adsorbed column density), in the years 1985 (left) and 1990 (right), just before and after equinox to show the 'ramp up' of exospheric density. Bottom: Model visualization showing the simulation CH_4 gas molecules and adsorbed methane polar cap.

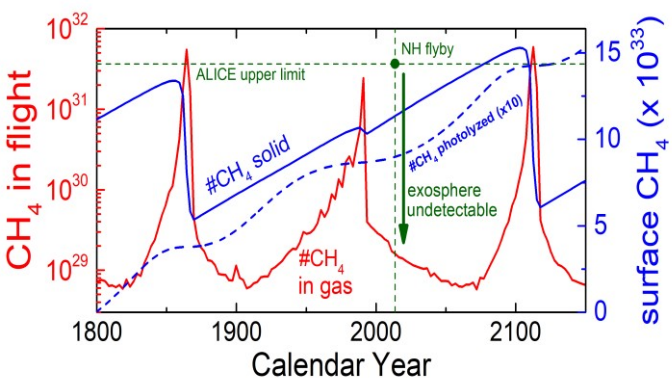

Figure 2. Total CH_4 molecules in the model exosphere (red) and on the surface (blue solid) versus time, and the cumulative number of CH_4 molecules photo-converted to surface photoproducts over one Pluto orbit (blue dashed). The predicted exospheric abundance is well below detectability [*Stern et al*., 2017] by New Horizons.

Acknowledgments: Work supported by the NASA New Frontier Data Analysis Program grant number 80NSSC18K1391.

References: [1] Stern, S. A., et al. (2017), *Icarus*, 287, 124. [2] Hoey, W. A., S. K. Yeoh, L. M. Trafton, D. B. Goldstein, and P. L. Varghese (2017), *Icarus*, 287, 87. [3] Tucker, O. J., R. E. Johnson, and L. A. Young (2015), *Icarus*, 246, 291. [4] Grundy, W. M., et al. (2016), *Nature* 539, 65. [5] Teolis, B. D. and Waite, J. H. (2016), Icarus, 272, 277. [6] Raut, U., B. D. Teolis, J. Kammer, C. Gimar, C. Howett, G. R. Gladstone, K. D. Retherford (2022), submitted.